

# Identify Microstructure and Mechanical Behavior of Aluminum Hybrid Nano Composite Prepared by Casting Technique

Khaldun Aldawoudi<sup>1</sup>, Ayad Mohammed Nattah<sup>2</sup>, Nabaa Sattar Radhi<sup>3</sup>,  
Zainab S. Al-Khafaji<sup>4,5\*</sup>, Manar Khaleel Ibrahim<sup>6</sup>

<sup>1</sup>College of Materials Engineering, University of Babylon, Babylon, Iraq

<sup>2</sup>College of Materials Engineering, University of Babylon, Babylon, Iraq

<sup>3</sup>College of Materials Engineering, University of Babylon, Babil, Iraq

<sup>4</sup>Department of Civil Engineering, Faculty of Engineering and Built Environment, Universiti Kebangsaan Malaysia, 43600 UKM Bangi, Selangor, Malaysia.

<sup>5</sup>Imam Ja'afar Al-Sadiq University, Baghdad, Iraq

<sup>6</sup>College of Materials Engineering, University of Babylon, Babylon, Iraq

Received 26 Sep 2024

Accepted 7 Jan 2025

## Abstract

The development of Aluminum-based composite metallic matrices (AMMCs) has become one of the main requirements for engineering applications due to their low weight, high strength, and superior mechanical characteristics. In this work, the effect of adding 1.25 wt% SiO<sub>2</sub>, 1.25 wt% Fe<sub>2</sub>O<sub>3</sub>, or a mixture of 1.25 wt% SiO<sub>2</sub> and 1.25 wt% Fe<sub>2</sub>O<sub>3</sub> hybrid particles on the hardness and compressive strength of an aluminum matrix composite fabricated by stir casting will be studied. A scanning electron microscope was utilized to investigate the microstructure of the specimens. Measurements of hardness and compressive strength characteristics revealed an improvement with increasing reinforcement weight percentage. Results for specimens of reinforced aluminum with 1.25 SiO<sub>2</sub>, 1.25 Fe<sub>2</sub>O<sub>3</sub>, or a mixture of 1.25 SiO<sub>2</sub> and 1.25 Fe<sub>2</sub>O<sub>3</sub> wt% particles indicated that the increment percentage of Brinell hardness was, respectively, 25.5%, 6.8%, and 19.3%. Finally, with an increasing percentage of iron or silicon oxide, the yield point and young modulus significantly decreased, even reaching the minimum magnitude at the composite containing 1.25% Fe<sub>2</sub>O<sub>3</sub> and 1.25% SiO<sub>2</sub>.

© 2025 Jordan Journal of Mechanical and Industrial Engineering. All rights reserved

**Keywords:** Aluminum Matrix Composites (AMCs), Fe<sub>2</sub>O<sub>3</sub>, SiO<sub>2</sub> hybrid particles, stir casting method, reinforcement, and Brinell hardness.

## 1. Introduction

A "composite" is a material system that consists of a distinct component (the reinforcement) dispersed in a continuous phase (the matrix) [1]–[9]. A composite's unique characteristics come from its components' characteristics, the arrangement and structure of the components, and the characteristics of the interfaces between the various components [10], [11]. Composite materials are often categorized based on the physical or chemical characteristics of the matrix phase, such as ceramic composites, metal-matrix, and polymer matrix [12]–[14]. Furthermore, studies have suggested the creation of Inter metallic-matrix and carbon-matrix composites. The literature has extensively examined metal matrix composites, particularly aluminum matrix composites (AMCs). [15], [16]. One of the constituents of AMCs is aluminum or an aluminum alloy, which forms a percolating network and is referred to as the matrix phase. The second component is included in the

aluminum/aluminum alloy structure and acts as reinforcement, often non-metallic and ceramic, including SiC and Al<sub>2</sub>O<sub>3</sub>[17]. The characteristics of AMCs may be customized by changing the composition and volume fraction of their components [18]–[20]. Using aluminum composite has proven to be increasingly efficient in various sectors, including but not limited to construction and automotive industries. Silicon carbide, alumina oxide, tungsten carbide, and titanium carbide are widely recognized as the most frequently utilized materials for reinforcing aluminum composites[21]. In the past few years, novel materials such as fullerene, graphene, and carbon nanotubes have been employed as enhancers for additives [22]. Figure 1 illustrates the several matrix and reinforcing materials that may be utilized to produce Metal Matrix Composites (MMCs). The many inorganic reinforcements, including borides (including titanium boride and zirconium boride), nitrides (such as titanium nitride), carbides (including silicon carbide and titanium carbide), and oxides (including aluminum oxide, titanium

\* Corresponding author e-mail: p123005@siswa.ukm.edu.my.

oxides, and zirconium oxides) are widely utilized but come with a somewhat high cost. The use of organic reinforcements, including red mud and fly ash, dramatically enhances the strength of the composite material while maintaining a relatively cheap cost [23], [24].

Composites, comprising a matrix and dispersed fibers, exhibit superior mechanical properties. Fibers, such as carbon or glass, act as the load-bearing phase, enhancing tensile strength, stiffness, and toughness, while the matrix ensures load transfer, structural cohesion, and environmental protection. Fibers interrupt crack propagation, enabling anisotropic properties and high strength-to-weight ratios critical in aerospace and automotive applications. Their incorporation significantly improves thermal stability, chemical resistance, and durability, providing a cost-effective solution for advanced material performance in demanding environments. The use of particulates in producing AMMCs is of paramount importance, as they are easily accessible, cost-effective, and more readily dispersible within the matrix. The most often utilized reinforcing particles in the micro to nano size range are  $\text{Al}_2\text{O}_3$ ,  $\text{B}_4\text{C}$ , and  $\text{SiC}$ . Adding these strengthening particles enhances the elastic modulus and

hardness while improving wear resistance [26].  $\text{SiC}$  is included in the mixture for its exceptional thermal characteristics, stiffness, specific strength, and hardness. On the other hand,  $\text{Al}_2\text{O}_3$  demonstrates impressive resistance to wear and compressive strength. Boron carbide is an exceptionally durable element with a high elastic modulus and resistance to fracture [27].

Using Iron oxide ( $\text{Fe}_3\text{O}_4$ ) as a reinforcement for aluminum matrix composites has gained significant attention in structural applications such as automotive and aeronautical. The substance exhibits exceptional ratios of strength-to-weight, stiffness-to-weight, and magnetic permeability. Furthermore, this material exhibits outstanding wear resistance and a reduced thermal expansion coefficient. Additionally, it exhibits superior thermal conductivity. Moreover, the unique attributes of this substance render it suitable for versatile applications owing to its low weight [28]. Aluminium and its alloys have better mechanical features and low densities and have now become utilized effectively in several applications [29]. A fundamental study has been undertaken on aluminum alloys to enhance specific properties such as mechanical, fatigue life, and corrosion resistance [30], [31].

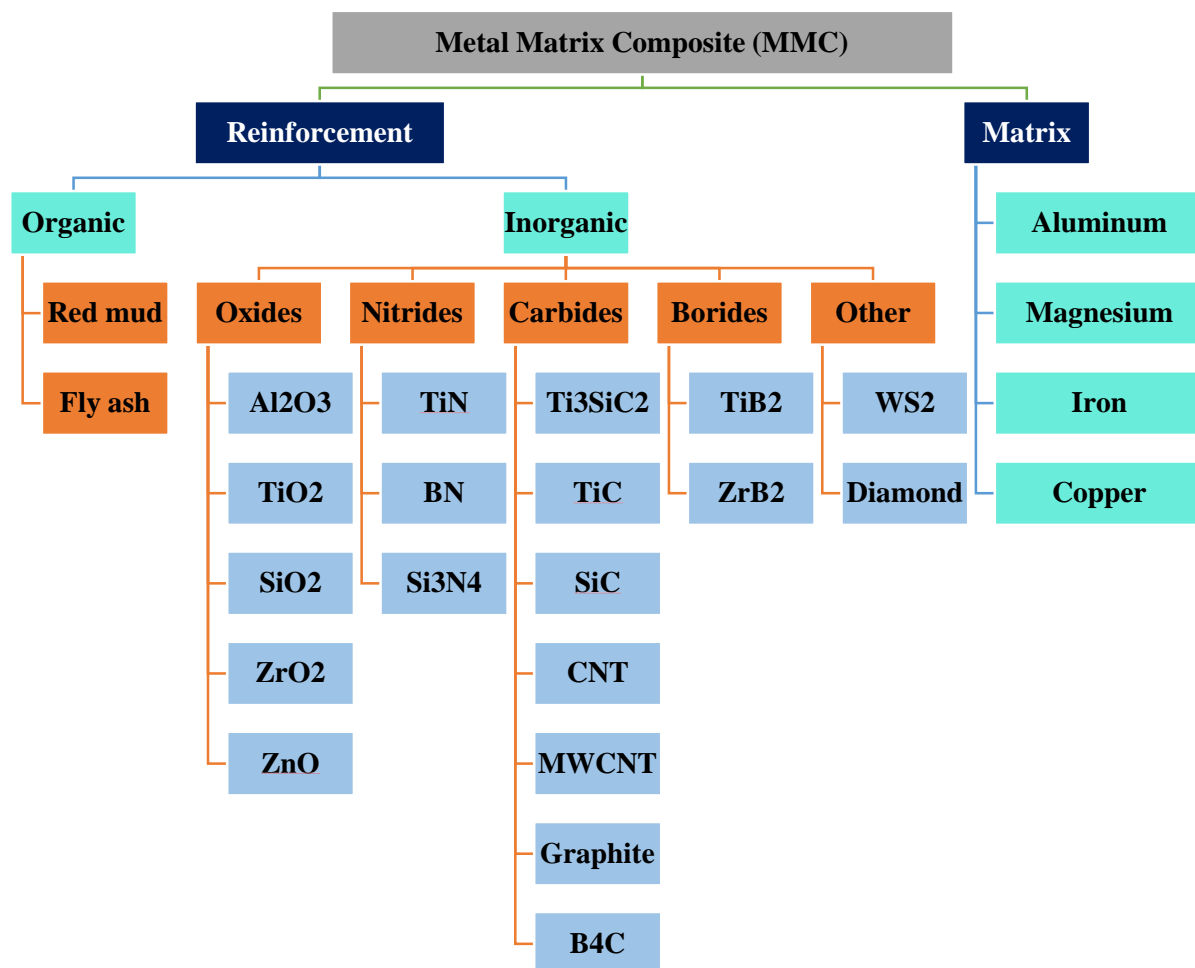


Figure 1. Various matrix and strengthening materials are utilized for MMC production [25].

Malakar et al. [32] utilized hybrid AMC by powder metallurgy. Varieties of reinforcement are incorporated into the composite to enhance its properties. Fly ash is mainly utilized as reinforcement. Approximately 10% of the weight of fly ash is incorporated into each composite. An additional 5% of the composite's total weight is allocated as alumina particles or  $\text{Al}_2\text{O}_3$  for fixed reinforcement. The weight percentages of  $\text{Fe}_2\text{O}_3(\text{III})$   $\text{Fe}_2\text{O}_3$  are altered by 1%, 2%, 3%, and 4% of the composite. Suaad M Jiaad et al. [33] successfully utilized the powder metallurgy method to make Ni hybrid Nano-composite +  $\text{Al}/\text{Fe}_3\text{O}_4$ . At various amounts of iron oxide  $\text{Fe}_3\text{O}_4$  from (2, 4, 6, 8, and 10) wt.% with Ni at a constant amount of 2 wt.% for preparation of the samples. The results indicated that hybrid nano-composite at increasing  $\text{Fe}_3\text{O}_4$  weight percentages increased the resistivity and the saturation magnetization ( $M_s$ ) magnitudes while the electrical conductivity decreased. The Field Emission Scanning Electron Microscopy analysis revealed a homogenous distribution of  $\text{Fe}_3\text{O}_4$  and Ni nanoparticles within the Al matrix. X-ray diffraction (XRD) study illustrated that the intensity of phase peaks  $\text{Fe}_3\text{O}_4$  and Ni increases when the weight % of  $\text{Fe}_3\text{O}_4$  increases while maintaining a constant amount of Ni.

Radhi et al., [34], [35] utilized powder metallurgy technology to prepare composite specimens of aluminum by adding  $\text{Fe}_2\text{O}_3$  nanoparticles at different weight ratios (2, 4, 6, and 8 wt%). The specimen preparation conditions included a blending time of 2 hours for each specimen, a compaction load of 6 tons, and a sintering temp of 600 degrees centigrade. The performed tests included XRD, SEM, EDS, green density measurement, green porosity analysis, microhardness testing, compression testing, and wear testing. The findings demonstrate that the hardness and wear magnitude exhibit an upward trend as the hematite % increases.

This study distinguishes itself from previous research by exploring the synergistic effects of hybrid nano-sized reinforcements, specifically  $\text{SiO}_2$  and  $\text{Fe}_2\text{O}_3$  particles, within an aluminum matrix composite (AMC). Unlike earlier studies that primarily focused on single-particle reinforcements, such as  $\text{Fe}_2\text{O}_3$  or Ni [33]–[35], this research evaluates the combined contributions of  $\text{SiO}_2$  and  $\text{Fe}_2\text{O}_3$  to achieve balanced improvements in hardness, compressive strength, and wear resistance. The innovative use of nano-sized reinforcements enhances interfacial bonding and addresses limitations associated with micro-sized particles, predominantly employed in prior work [32]. Furthermore, the advanced stir-casting methodology employed in this study, featuring a two-step stirring process and preheating of particles, ensures superior particle dispersion compared to conventional powder metallurgy techniques [32], [33]. Unlike earlier studies that emphasized limited mechanical characterization, this research provides a comprehensive analysis encompassing Brinell hardness, compressive strength, and wear resistance, offering critical insights into the tribological performance of hybrid composites. The findings reveal intermediate mechanical properties between single-reinforced composites, confirming the efficacy of hybrid reinforcements in enhancing overall performance. These contributions address existing gaps in the literature and pave the way for developing lightweight, high-

performance materials suitable for advanced engineering applications. This study introduces a novel approach to developing aluminum hybrid nano-composites by integrating nano-sized silicon oxide ( $\text{SiO}_2$ ) and iron oxide ( $\text{Fe}_2\text{O}_3$ ) as reinforcements into a pure aluminum matrix using the stir casting technique. While previous research predominantly explored single-particle reinforcement in aluminum matrices, this study delves into the synergistic effects of hybrid nano-reinforcements on microstructure and mechanical behavior, a relatively underexplored area in the literature. The research employs a two-step stir-casting process combined with the preheating of reinforcement particles to overcome challenges related to wettability and distribution, ensuring a homogenous composite structure. The study provides comprehensive insights into how different reinforcement compositions influence composite behavior by evaluating the microstructure using SEM and XRD, alongside mechanical tests such as Brinell hardness, compressive strength, and wear tests. This research aims to fabricate, identify, and characterize the mechanical behavior and hardness of (AMC) reinforced with nano Hematite, nano silicon oxide, hybrid nano Hematite, and nano silicon oxide. The novelty of this study lies in developing and characterizing hybrid aluminum matrix composites (AMCs) reinforced with nano-sized  $\text{SiO}_2$  and  $\text{Fe}_2\text{O}_3$  particles, fabricated using an advanced two-step stir-casting method. Unlike prior studies focusing on single reinforcements, this research evaluates the synergistic effects of hybrid particles on mechanical and tribological properties. The study introduces a unique preheating and dispersion technique to ensure uniform particle distribution, enhancing hardness, compressive strength, and wear resistance. This work fills a critical gap in the literature by providing a comprehensive understanding of hybrid nano-reinforcements in AMCs for advanced engineering applications.

## 2. Experimental Work

### 2.1. Preparation of AMMC specimens

Table 1 lists all AMMC specimens that were created using high-purity aluminum wires.

**Table 1:** Pure aluminum with chemical composition

Element	*Cu	Fe	Si	Mn	Zn	Mg	Others total
%	1	12	6	1	3	2	10

Different reinforcing percentage samples were produced utilizing the two-step stir-casting procedure. The specimen compositions are displayed in Table 2.

**Table 2:** The specimens presented in this work.

Specimens	Al wt%	Mg wt%	$\text{SiO}_2$ wt%	$\text{Fe}_2\text{O}_3$ wt%
Al- $\text{SiO}_2$	96.75	2	1.25	-
Al- $\text{Fe}_2\text{O}_3$	96.75	2	-	1.25
Al- $\text{SiO}_2$ - $\text{Fe}_2\text{O}_3$	95.5	2	1.25	1.25

The small pieces were prepared by cutting high-purity aluminum wires to prepare them for the melting process in the furnace. The grain size for each silicon oxide, aluminum wire, iron oxide, and magnesium are 15-20  $\mu\text{m}$ . The samples were prepared in the desired amount (weight

percentage wt%). Then, in a dry oven type (SRJX-5-13), an aluminum foil was preheated up to (300 °C) for 2 hours to cover each group. This process enhances the wettability and removes the moisture content. The pieces of aluminum wire to be placed in the gas furnace were charged in the graphite crucible. The oven temp was increased to 750°C, the liquidus temperature, to completely melt the aluminum. An alumina spoon was utilized to remove the slags. To reach the semi-solid state, the melting temperature dropped to (620°C), just below the liquid temperature. A thick aluminum foil was folded and placed over the magnesium ribbon before dipping it under the melt to reduce its combustion. The mechanical mild steel stirrer stirred molten aluminum slurry for 7 min at 870 rpm. It is covered with preheated silicon oxide, iron oxide particles, or both as the plain, gently adding to the metal. The stirring process must be set up under an argon gas shield to prevent molten aluminum from oxidizing. The composite strength and particle distribution depend mainly on the stirrer blade design. Microstructure analysis for composite manufactured with a four-blade stirrer shows adequate particle distribution.

The temperature was measured with a thermocouple kind-K at (610-620) degrees centigrade while the melted mixture was stirred. Next, an increase in temperature above the liquidus temperature of 750°C. The molten composite is stirred simultaneously and at a consistent speed at the liquidus temperature. Finally, place the molten composite into a warmed steel mold for solidification. Composite casts were made as each percentage increased. The aluminum was cast without adding any reinforcing particles in the comparison procedure. A heat treatment at (350°C) for (5 hours) was employed for samples to relieve the thermal stresses and homogenization. Then, the physical and mechanical tests are ready for composite samples.

## 2.2. The physical Tests

### 2.2.1. Scanning Electron Microscope Examination

Specimens were cut from each rod at (13 mm) in diameter. The grinding with sandpapers having different SiC grits (180, 320, 400, 800, 1000, 1500, 2000, 2500) were employed on the AMMC specimens. The temperature in the grinding operation increases because of the friction between the sample and the grinding papers. Thus, a coolant must be used to avoid elevated temperatures during the grinding process, and the water was utilized for this purpose. Then, the diamond paste was used to polish specimens to produce flat, scratch-free, surface-like mirrors. The polishing machine model (MP-2B grinder polisher) performed the grinding and polishing operations. The specimens were etched at room temp using a mix of 99.5% distilled water and 0.5% hydrofluoric acid for 15 seconds [36]. Distilled water was used to wash the specimens, which must be placed in the electric dryer. The microstructure of each specimen was identified by scanning electron microscope.

### 2.2.2. The X-Ray Diffraction Analysis

X-ray diffraction (XRD) analysis is an important technique for identifying the compositions and crystalline phases in the specimens produced. This analysis was

performed by scanning all selected specimens for possible diffraction directions through a range of  $2\theta$  angles from  $10^\circ$  to  $90^\circ$ . The operation conditions of XRD were target current (20  $\mu$ A), voltage (40 KV), wavelength of 1.54060 Å, and Cu.

## 2.3. The Mechanical Tests

### 2.3.1. The Brinell Hardness Test

ASTM (E10-15a) states that a Brinell test sample has no standardized size or shape. Each rod was utilized to cut a specimen of a specific size, which was then polished and ground accordingly. A Brinell hardness testing apparatus of type HBRVS-187.5 with a 5mm ball indenter diameter and a 31.25 Kg force applied for 10 seconds was utilized for the test. Hardness magnitudes were recorded for each specimen by calculating the mean of three measurements.

### 2.3.2. Compression Test

Cylindrical samples with dimensions (12 mm diameter and 24 mm height) were utilized for compression tests. According to the ASTM standard (L=2D), the specimens were prepared [37]. The traditional machining operations were conducted to prepare cylindrical samples with standard dimensions. All compression tests were carried out at room temperature using an automated common testing machine type (United Test, China) with a loading ratio of (0.1 mm/min).

### 2.3.3. The Wear Test

The composite specimens were made with a diameter of 12 mm and a height of 5 mm according to ASTM (G99-17) [38]. The samples in previous tests were polished using silicon carbide (SiC) sheets until they achieved an average surface roughness of 0.5  $\mu$ m. The vacuum furnace was preheated to 100°C for 30 minutes to dry the specimens after cleaning. This method enables the complete removal of any cleaning fluids that might be trapped in the material. A precise electric balance model (M254A) with an accuracy of +0.0001 was employed for weighing. The research on dry wear was conducted using the wear tester equipment model MT-4003, version 10.0, which operates on the pin-on-disk idea. The pin was positioned against a standard revolving steel disk for testing specimens with a hardness of 850 HV. The normal force on the pin is 10 N, the pin diameter is 10 mm, the disk diameter is 30 mm, the worn track radius is 5 mm, and the rotating speed of the disk is 300 rpm. The specimen was weighed after 5, 10, 15, and 20 minutes to evaluate the weight loss. Next, convert the weight loss to volume loss using the following equation [39]:

$$\text{Volume loss (mm}^3\text{)} = \text{weight loss (g)} / \text{density (g/mm}^3\text{)} \quad (3)$$

Where: weight loss = weight before the test – weight after the test.

Volume loss (mm<sup>3</sup>) is calculated by dividing the weight loss (g) by the density (g/mm<sup>3</sup>).

The formula for weight loss is calculated by subtracting the weight after the test from the weight before the test.

## 3. Results and Discussion

### 3.1. Scanning Electron Microscope Analysis

Manufacturing metal-matrix composites by casting techniques, including silica and hematite, and combining both particles. The challenge arises from the limitation of

particle wettability and aggregation, leading to substandard mechanical qualities and uneven distribution. This study prepared aluminum alloy matrix composites using nano-sized silica, hematite, and a mixture of both particles by the stir-casting method. A unique three-stage mixing process and preheated reinforcing particles were employed. The composites had silica, hematite, and a mixture of both particles in powder form at a weight percentage of 1.25% SiO<sub>2</sub>, 1.25% Fe<sub>2</sub>O<sub>3</sub>, and 1.25% SiO<sub>2</sub> + 1.25% Fe<sub>2</sub>O<sub>3</sub>. Figure 2(a-c) reveals the scanning electron microscope images

### 3.2. X-Ray Diffraction Analysis

Every sample underwent X-ray diffraction analyses to identify the nano-composite specimens used in this project. These studies provide findings that are shown in Figure 3. To find the phases already existing in every sample, an X-ray diffraction test was performed on 1.25 wt% of Fe<sub>2</sub>O<sub>3</sub> and 1.25 wt% of SiO<sub>2</sub> nano powders implanted in the aluminum matrix. The diffraction angle (2θ°) spans (30 to 80)°, and the phases generated by this range are covered further. Once comparing the XRD findings, one finds displaced aluminum peaks for Fe<sub>2</sub>O<sub>3</sub> and SiO<sub>2</sub>.

### 3.3. Brinell Hardness Test Analysis

The Brinell hardness test illustrated the findings as demonstrated in Figure 4. It is specified that with the addition of Fe<sub>2</sub>O<sub>3</sub> particles of (1.25 wt%), the hardness is increased and recorded at 22.5. The highest magnitude for specimens with silicon oxide percentage of (1.25 wt%) was recorded at 24.1, while the hardness magnitude between them when mixed (1.25 wt%) SiO<sub>2</sub> and (1.25 wt%) Fe<sub>2</sub>O<sub>3</sub>. It is concluded that this increment referring to the hardness of oxide particles is high enough to work as a barrier against dislocation movement. The Brinell hardness shows the increment percentage at (25.5%), (6.8%) and (19.3%) for aluminum reinforced with (1.25 SiO<sub>2</sub>, 1.25 Fe<sub>2</sub>O<sub>3</sub> and 1.25 SiO<sub>2</sub>- 1.25 Fe<sub>2</sub>O<sub>3</sub>)wt. % of particle specimens respectively compared with nonreinforced specimens. The results show a good agreement with the mixture role if silicon oxide has higher hardness than Fe<sub>2</sub>O<sub>3</sub> references [40], [41] with differences at acceptable magnitudes according to the variation in chemical composition and the mean size of strengthening utilized and Al-alloy[42], [43].

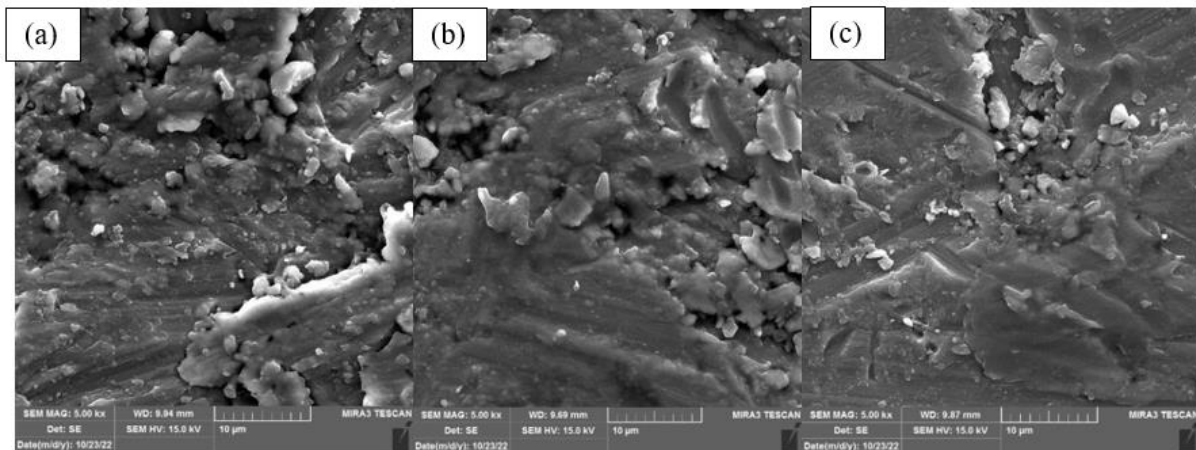


Figure 2. SEM a) 1.25 wt%Fe<sub>2</sub>O<sub>3</sub>, b) 1.25 wt%SiO<sub>2</sub>, c)1.25 wt%Fe<sub>2</sub>O<sub>3</sub>+1.25 wt%SiO<sub>2</sub>.

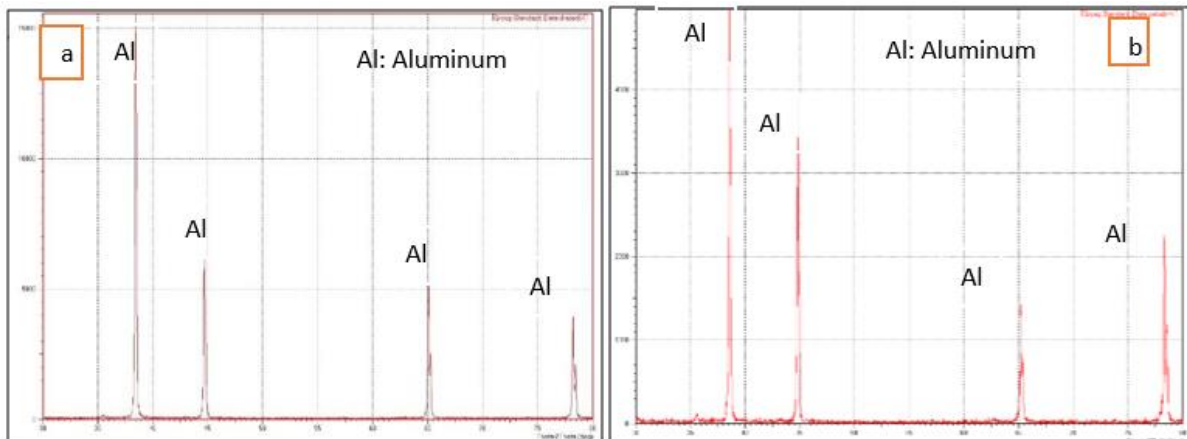


Figure 3. XRD pattern of a: Al-(1.25 wt.%) Fe<sub>2</sub>O<sub>3</sub> b: Al-(1.25 wt.%) SiO<sub>2</sub>.

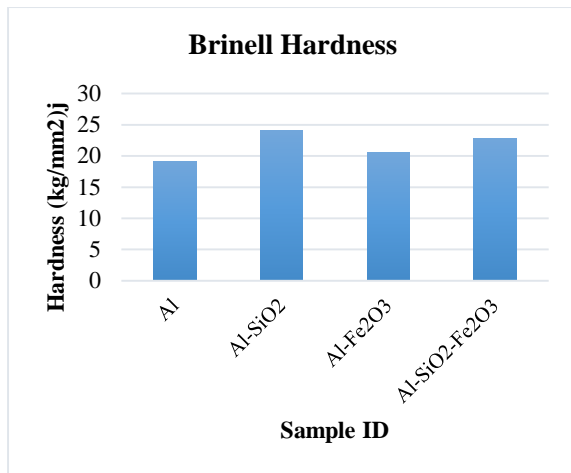


Figure 4. The Brinell hardness magnitude for different Al alloys.

### 3.4. The compressive strength test analysis

The reinforcing effects of the added SiO<sub>2</sub> and Fe<sub>2</sub>O<sub>3</sub> particles can justify the compressive strength results of the aluminum (Al) alloys. Pure aluminum exhibits the lowest compressive strength due to its soft and ductile nature, lacking secondary phases to impede dislocation motion. Adding 1.25% SiO<sub>2</sub> significantly enhances the compressive strength by introducing a rigid ceramic phase that obstructs dislocation movement, improving load-bearing capacity. On the other hand, the addition of 1.25% Fe<sub>2</sub>O<sub>3</sub> yields the highest compressive strength, attributed to the formation of intermetallic Al-Fe phases, which are mechanically rigid and provide strong interface bonding, ensuring effective stress transfer during compression[44]. When SiO<sub>2</sub> and Fe<sub>2</sub>O<sub>3</sub> are combined at 1.25% each, the compressive strength is slightly lower than Fe<sub>2</sub>O<sub>3</sub> alone, possibly due to competition between the two additives during processing, leading to slight agglomeration or suboptimal phase distribution[45]. Overall, the results indicate that both SiO<sub>2</sub> and Fe<sub>2</sub>O<sub>3</sub> significantly enhance the mechanical properties of aluminum, with Fe<sub>2</sub>O<sub>3</sub> showing the most pronounced effect due to its ability to form intermetallic phases. At the same time, their combination offers a balanced approach to improving the alloy's performance[46].

Figure 6 demonstrates that increasing the proportion of Fe<sub>2</sub>O<sub>3</sub> in the aluminum base improved compressive strength. The enhancement in compressive strength is attributed to the effective role of Fe<sub>2</sub>O<sub>3</sub> particles. These functioned as barriers that impeded the dislocation motion, strengthening the matrix. Adding magnesium to the aluminum matrix enhances the contact link between the aluminum matrix and silicon oxide particles, resulting in a substantial bonding enhancement. The compressive strength of the Al+ 1.25% Fe<sub>2</sub>O<sub>3</sub> specimen showed a maximum increase of 165% compared with the pure aluminum. Figure (6) shows the Young's modulus of these composite materials samples. Where the value of Young's modulus of the pure aluminum was (73 Gpa), while that decreasing Young modulus value with increasing reinforcement percentage was (47 Gpa) for Al+(1.25 SiO<sub>2</sub>+1.25 Fe<sub>2</sub>O<sub>3</sub>), the rest of the values for other samples fall between these two values. The Young's modulus of the

(Al+1.25 SiO<sub>2</sub>) sample is (63 Gpa), and (Al+ 1.25 Fe<sub>2</sub>O<sub>3</sub>) is (60 Gpa). This value is lower than the modulus of elasticity value for aluminum.

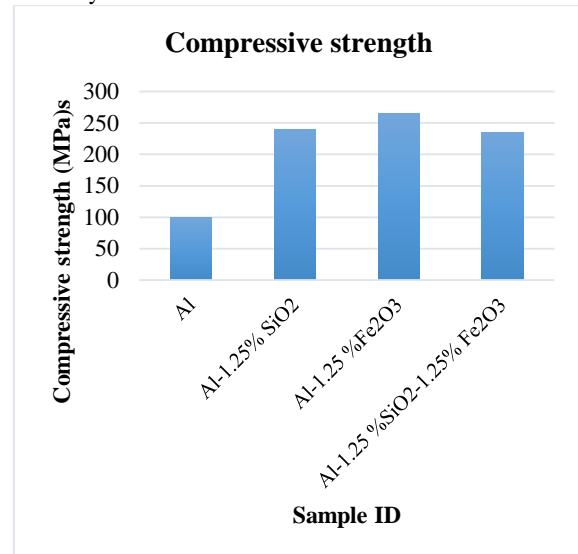


Figure 5: Compressive strength magnitude of different Al alloys.

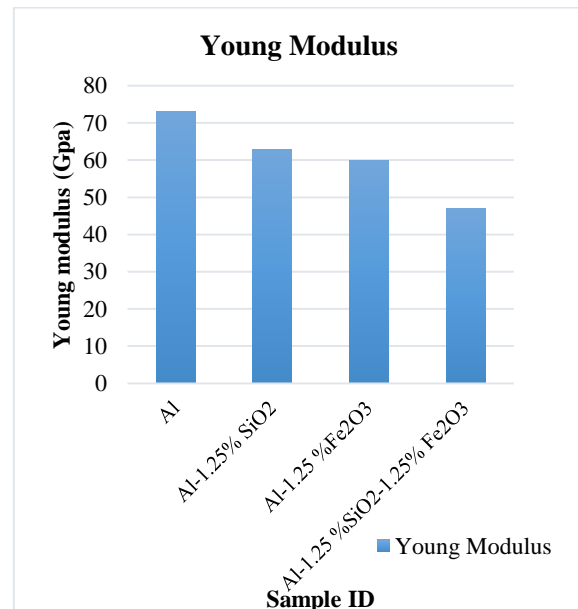


Figure 6: Shows the Young modulus vs Al percentage.

### 3.5. The wear tests Analysis

By selecting the density of each sample, it is possible to transform the weight loss into a corresponding volume loss. Figure 7 illustrates the findings of the test conducted under the same specific circumstances as previously described (F: 10 N;  $\omega$ : 300 rpm; t: 5, 10, 15, and 20 min). Figure 7 shows that as the applied load increases, volume loss also increases; the maximum volume loss was noted under (10 N) and vice versa. Usually, the expected behavior involves increased friction between the sample surface and the rotating disk as the load increases. Over time, the volume loss increased due to the particles being lost from the specimen as friction time increased.

Furthermore, the impact of incorporating Fe<sub>2</sub>O<sub>3</sub> particles under various settings on wear rates is

demonstrated in these data. The volume loss decreased dramatically as the proportion of  $\text{Fe}_2\text{O}_3$  increased, reaching its most minor magnitude in the composite, with the highest percentage of  $\text{Fe}_2\text{O}_3$  (1.25%). This happens due to the influential role of  $\text{Fe}_2\text{O}_3$  particles in impeding dislocation motion. The addition of silicon oxide and a combination of  $\text{Fe}_2\text{O}_3$  and silicon oxide hardness further enhance wear resistance. The wear resistance is improved by the presence of hard  $\text{Fe}_2\text{O}_3$  and  $\text{SiO}_2$  particles in the Al alloy, which prevents the ploughing action of the hard steel equivalent. The results are depicted in Figure 7.

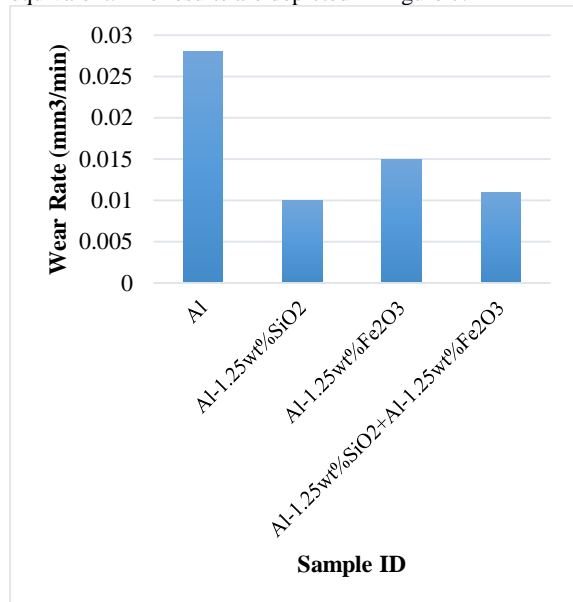


**Figure 7:** At steady state, the wear rate for Al specimens at (time=20 min.).

#### 4. Conclusion

The current study used the stir casting technique to produce Al- $\text{SiO}_2$ , Al- $\text{Fe}_2\text{O}_3$ , and Al-( $\text{SiO}_2+\text{Fe}_2\text{O}_3$ ) composites. The compressive strength, hardness, and wear behavior were evaluated to observe how particle dispersion and these characteristics grow with a higher weight percentage of  $\text{Fe}_2\text{O}_3$ .

1. SEM and XRD results show the nanoparticles impeded in the aluminum matrix and shifting the peaks of the XRD pattern.
2. The finding illustrated that at 10 N, the highest wear rate is in the Al sample, and the wear rate is reduced by (46.4) % in aluminum reinforced by 1.25 %  $\text{Fe}_2\text{O}_3$ .
3. The percentage increment of Brinell hardness is (25.5%), (6.8%) and (19.3%) for aluminum reinforced with 1.25  $\text{SiO}_2$ , 1.25  $\text{Fe}_2\text{O}_3$ , and (1.25  $\text{SiO}_2$ , 1.25  $\text{Fe}_2\text{O}_3$ ) wt. % particles specimens, respectively.
4. The maximum improvement for the Al+1.25  $\text{Fe}_2\text{O}_3$  specimen was recorded at 26.5 % in compressive strength.
5. The young modulus values decrease with an increasing reinforcement percentage.

Further optimization of stir-casting parameters is recommended to enhance particle wettability and minimize agglomeration, while exploring different weight percentages and hybrid reinforcement combinations could provide a more balanced improvement in mechanical

properties. Additionally, fatigue testing and long-term environmental exposure studies are essential for assessing durability. However, the stir-casting method has limitations in achieving uniform nanoparticle dispersion compared to advanced techniques like additive manufacturing. The study was also limited to room-temperature performance, necessitating future evaluations under varying thermal and mechanical conditions. Moreover, the high cost of nano-reinforcements remains a significant challenge for large-scale industrial applications.

#### References

- [1] D. K. Rajak, D. D. Pagar, R. Kumar, and C. I. Pruncu, "Recent progress of reinforcement materials: a comprehensive overview of composite materials," *Journal of Materials Research and Technology*, vol. 8, no. 6, pp. 6354–6374, 2019.
- [2] M. Balasubramanian, *Composite materials and processing*, vol. 711. CRC press Boca Raton, 2014.
- [3] A. H. Haleem, N. S. Radhi, N. T. Jaber, and Z. Al-Khafaji, "Preparation and Exploration of Nano-Multi-Layers on 316L Stainless Steel for Surgical Tools," *Jordan Journal of Mechanical and Industrial Engineering (JJMIE)*, vol. 18, no. 2, 2024.
- [4] M. R. Jasim, Y. Alaiwi, and Z. Al-khafaji, "Investigation Of The Effect Of Adding Nitrogen On The Torque Generated By A Four-Cylinder Engine," *Jordan Journal of Mechanical and Industrial Engineering*, pp. 1–30, 2024.
- [5] Ł. J. Orman, "Enhanced Boiling Heat Transfer on Surfaces Covered with Microstructural Mesh Coatings.," *Jordan Journal of Mechanical and Industrial Engineering*, vol. 13, no. 3, pp. 155–160, 2019.
- [6] A. Ismail, R. Zenasni, K. S. M. Amine, and S. Ahmed, "Effect of tempering temperature on the mechanical properties and microstructure of low alloy steel DIN 41Cr4," *Jordan Journal of Mechanical and Industrial Engineering*, vol. 13, no. 1, pp. 9–14, 2019.
- [7] R. M. K. Ali and S. L. Ghashim, "Thermal performance analysis of heat transfer in pipe by using metal foam.," *Jordan Journal of Mechanical & Industrial Engineering*, vol. 17, no. 2, pp. 205–218, 2023.
- [8] A. R. I. Kheder, N. M. Jubeh, and E. M. Tahah, "Fatigue Properties under Constant Stress/Variable Stress Amplitude and Coaxing Effect of Acicular Ductile Iron and 42 CrMo4 Steel.," *Jordan Journal of Mechanical and Industrial Engineering*, vol. 5, no. 4, pp. 301–306, 2011.
- [9] S. Dwivedi and S. Sharma, "Optimization of Resistance Spot Welding Process Parameters on Shear Tensile Strength of SAE 1010 steel sheets Joint using Box-Behnken Design.," *Jordan Journal of Mechanical and Industrial Engineering*, vol. 10, no. 2, pp. 115–122, 2016.
- [10] V. V. Vasiliev and E. V. Morozov, *Advanced mechanics of composite materials and structures*. Elsevier, 2018.
- [11] H. Altenbach, J. Altenbach, W. Kissing, and H. Altenbach, *Mechanics of composite structural elements*. Springer, 2004.
- [12] A. Mortensen and J. Llorca, "Metal matrix composites," *Annual review of materials research*, vol. 40, no. 1, pp. 243–270, 2010.
- [13] K. K. Chawla, *Ceramic matrix composites*. Springer Science & Business Media, 2013.
- [14] R. N. Hwayyin and A. S. Ameen, "The Time Dependent Poisson's Ratio of Nonlinear Thermoviscoelastic Behavior of Glass/Polyester Composite.," *Jordan Journal of Mechanical and Industrial Engineering*, vol. 16, no. 4, pp. 515–528, 2022.
- [15] S. T. Mavhungu, E. T. Akinlabi, M. A. Onitiri, and F. M. Varachia, "Aluminum matrix composites for industrial use:

- advances and trends,” *Procedia Manufacturing*, vol. 7, pp. 178–182, 2017.
- [16] M. H. Rahman and H. M. M. Al Rashed, “Characterization of silicon carbide reinforced aluminum matrix composites,” *Procedia Engineering*, vol. 90, pp. 103–109, 2014.
- [17] M. B. N. Shaikh, S. Arif, T. Aziz, A. Waseem, M. A. N. Shaikh, and M. Ali, “Microstructural, mechanical and tribological behaviour of powder metallurgy processed SiC and RHA reinforced Al-based composites,” *Surfaces and Interfaces*, vol. 15, pp. 166–179, 2019.
- [18] D. Manfredi *et al.*, “Additive manufacturing of Al alloys and aluminium matrix composites (AMCs),” *Light metal alloys applications*, vol. 11, pp. 3–34, 2014.
- [19] Y. Wang and T. Monetta, “Systematic study of preparation technology, microstructure characteristics and mechanical behaviors for SiC particle-reinforced metal matrix composites,” *Journal of Materials Research and Technology*, vol. 25, no. 1, pp. 7470–7497, 2023.
- [20] A. M. Nattah, K. E. F. Aldawoudi, and E. M. S. Salih, “Effects of Nano particles of (Al<sub>2</sub>O<sub>3</sub>, Fe<sub>2</sub>O<sub>3</sub>) as Reinforcement on Mechanical Properties of Aluminum,” *Journal of University of Babylon for Engineering Sciences*, pp. 59–71, 2023.
- [21] M. B. N. Shaikh, S. Arif, and M. A. Siddiqui, “Fabrication and characterization of aluminium hybrid composites reinforced with fly ash and silicon carbide through powder metallurgy,” *Materials Research Express*, vol. 5, no. 4, p. 46506, 2018.
- [22] M. S. Fuhaid, R. V. Murali, M. A. Maleque, P. K. Krishnan, and M. A. Rahaman, “Synthesis and Characterization of Aluminium Composite with Graphene Oxide Reinforcement,” in *IOP Conference Series: Materials Science and Engineering*, IOP Publishing, 2021, p. 12005.
- [23] A. M. A. Abdo, “Utilizing Reclaimed Asphalt Pavement (RAP) Materials in New Pavements - A Review,” *International Journal of Thermal and Environmental Engineering*, vol. 12, no. 1, pp. 10–16, 2015, doi: 10.5383/ijtee.12.01.008.
- [24] K. S. Randhawa, “A state-of-the-art review on advanced ceramic materials: fabrication, characteristics, applications, and wettability,” *Pigment & Resin Technology*, 2023.
- [25] L. Singh, B. Singh, and K. K. Saxena, “Manufacturing techniques for metal matrix composites (MMC): an overview,” *Advances in Materials and Processing Technologies*, vol. 6, no. 2, pp. 441–457, 2020.
- [26] S. J. Huang, A. Abbas, and B. Ballóková, “Effect of CNT on microstructure, dry sliding wear and compressive mechanical properties of AZ61 magnesium alloy,” *Journal of Materials Research and Technology*, vol. 8, no. 5, pp. 4273–4286, 2019.
- [27] A. Ramanathan, P. K. Krishnan, and R. Muraliraja, “A review on the production of metal matrix composites through stir casting–Furnace design, properties, challenges, and research opportunities,” *Journal of Manufacturing processes*, vol. 42, pp. 213–245, 2019.
- [28] E. Bayraktar and D. Katundi, “Development of a new aluminium matrix composite reinforced with iron oxide (Fe<sub>3</sub>O<sub>4</sub>),” *Journal of achievements in materials and manufacturing engineering*, vol. 38, no. 1, pp. 7–14, 2010.
- [29] B. B. Verma, J. D. and Atkinson, and M. Kumar, “Study of fatigue behaviour of 7475 aluminium alloy,” *Bulletin of Materials Science*, vol. 24, pp. 231–236, 2001.
- [30] M. Jimenez-Martinez and M. Alfaro-Ponce, “Effects of synthetic data applied to artificial neural networks for fatigue life prediction in nodular cast iron,” *Journal of the Brazilian Society of Mechanical Sciences and Engineering*, vol. 43, no. 1, p. 10, 2021.
- [31] J. F. Barbosa, J. A. F. O. Correia, R. C. S. F. Júnior, and A. M. P. De Jesus, “Fatigue life prediction of metallic materials considering mean stress effects by means of an artificial neural network,” *International Journal of fatigue*, vol. 135, p. 105527, 2020.
- [32] S. Malakar, A. kumar Malaker, M. N. Islam, H. Karmaker, and A. Siddique, “Mechanical characterization of Aluminum Matrix Composite Reinforcement with Fly Ash, Al<sub>2</sub>O<sub>3</sub> and Fe<sub>2</sub>O<sub>3</sub>”.
- [33] S. M. Jiaad, K. D. Salman, and A. A. Hussein, “Evaluation the microstructure, physical, magnetic and electrical properties of Al/Fe<sub>3</sub>O<sub>4</sub>+ Ni hybrid nanocomposite,” in *Journal of Physics: Conference Series*, IOP Publishing, 2021, p. 12094.
- [34] N. S. Radhi, A. M. Nattah, and Z. S. Al-Khafaji, “Identify the effect of Fe<sub>2</sub>O<sub>3</sub> nanoparticles on mechanical and microstructural characteristics of aluminum matrix composite produced by powder metallurgy technique,” *Open Engineering*, vol. 14, no. 1, p. 20220519, 2024.
- [35] N. S. Radhi, A. H. Jasim, Z. S. Al-khafaji, and M. Falah, “Investigation of Hematite Nanoparticles According to Mechanical Characteristics of Aluminium Matrix Composite,” *Nanosistemi, Nanomateriali, Nanotehnologii*, vol. 21, no. 4, pp. 769–778, 2023.
- [36] A. J. Salman, “Experimental Analysis of In-situ Composite Al-Si Eutectic Alloy”.” MSc thesis, university of Babylon, 2009.
- [37] ASTM-E9, “Compression Testing of Metallic Materials at Room Temperature,” *ASTM International, West Conshohocken*, pp. 517–543, 2015.
- [38] W. Conshohocken, “ASTM G99-17, standard test method for wear testing with a pin-on-disk apparatus, ASTM International,” *Wear*, vol. 1, pp. 1–5, 2017.
- [39] N. M. Dawood, N. S. Radhi, and Z. S. Al-Khafaji, “Investigation corrosion and wear behavior of Nickel-Nano silicon carbide on stainless steel 316L,” in *Materials Science Forum*, Trans Tech Publ, 2020, pp. 33–43.
- [40] X. Ren, W. Zhang, Y. Zhang, P. Zhang, and J. Liu, “Effects of Fe<sub>2</sub>O<sub>3</sub> content on microstructure and mechanical properties of CaO–Al<sub>2</sub>O<sub>3</sub>–SiO<sub>2</sub> system,” *Transactions of Nonferrous Metals Society of China*, vol. 25, no. 1, pp. 137–145, 2015.
- [41] D. S. Ng *et al.*, “Influence of SiO<sub>2</sub>, TiO<sub>2</sub> and Fe<sub>2</sub>O<sub>3</sub> nanoparticles on the properties of fly ash blended cement mortars,” *Construction and Building Materials*, vol. 258, p. 119627, 2020.
- [42] K. Ma *et al.*, “Mechanical behavior and strengthening mechanisms in ultrafine grain precipitation-strengthened aluminum alloy,” *Acta Materialia*, vol. 62, pp. 141–155, 2014.
- [43] F. Bosio, P. Fino, D. Manfredi, and M. Lombardi, “Strengthening strategies for an Al alloy processed by in-situ alloying during laser powder bed fusion,” *Materials & Design*, vol. 212, p. 110247, 2021.
- [44] M. Nuthalapati, “Development of Nano-TiO<sub>2</sub>/Y<sub>2</sub>O<sub>3</sub> Dispersed Zirconium Alloys By Mechanical Alloying Followed By Conventional and Spark Plasma Sintering.” 2016.
- [45] A. Rozhkovskaya, “Synthesis of high quality zeolite from alum sludge for water treatment applications.” Queensland University of Technology, 2021.
- [46] M. S. L. Amirkhanyan, “Thermodynamic properties of intermetallics.” Technische Universität Bergakademie Freiberg Saxony, Germany, 2017.